The Importance of Nanocrystal Precursor Conversion Kinetics: Mechanism of the Reaction between Cadmium Carboxylate and Cadmium Bis(diphenyldithiophosphinate)

Mark P. Hendricks, Brandi M. Cossairt,[†] and Jonathan S. Owen[*]

Department of Chemistry, Columbia University, New York, New York 10027, United States. [†]Present address: Department of Chemistry, University of Washington, Seattle, Washington 98195, United States.

ABSTRACT We describe the synthesis of cadmium bis(diphenyldithiophosphinate) ($Cd(S_2PPh_2)_2$) from secondary phosphine sulfides and its conversion to cadmium sulfide nanocrystals. Heating $Cd(S_2PPh_2)_2$ and cadmium tetradecanoate ($\geq$4 equiv) to 240 °C results in complete conversion of $Cd(S_2PPh_2)_2$ to cadmium sulfide nanocrystals with tetradecanoate surface termination. The nanocrystals have a narrow size distribution (d = 3.8–4.1 nm, σ < 10%) that is evident from the line width of the lowest energy absorption feature (λ = 412–422 nm, fwhm = 0.17 eV) and display bright photoluminescence ($PLQY_{band\ \ edge+trap}$ = 36%). Interestingly, the final diameter is insensitive to the reaction conditions, including the total concentration of precursors and initial cadmium to sulfur ratio. Monitoring the reaction with ^{31}P NMR, UV–visible, and infrared absorption spectroscopies shows that the production of cadmium diphenylphosphinate ($Cd(O_2PPh_2)_2$) and tetradecanoic anhydride co-products is coupled with the formation of cadmium sulfide. From these measurements we propose a balanced chemical equation for the conversion reaction and use it to optimize a synthesis that affords CdS nanocrystals in quantitative yield. In light of these results we discuss the importance of well-defined precursor reactivity to reproducible conversion kinetics and the synthesis of nanocrystals with unambiguous chemical composition.

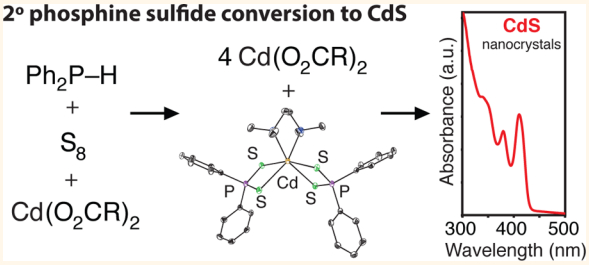

KEYWORDS: cadmium sulfide · nanocrystal synthesis · quantum dot synthesis · secondary phosphine chalcogenide · size distribution focusing · cadmium bis(diphenyldithiophosphinate) · growth kinetics

Solution-phase synthesis is a powerful method by which to control the size, shape, and composition of inorganic nanostructures.[1] This approach has recently been used to prepare numerous interesting structures, including two-dimensional crystals of II–VI and IV–VI materials,[2,3] heterostructures with graded interfaces,[4,5] seeded rod- and tetrapod shapes,[6,7] and transition-metal-doped nanocrystals with control over the location of dopant atoms.[8] Control over synthetic conditions can be used to tune energy level structure and the resultant recombination dynamics such as photoluminescence blinking,[9,10] Auger processes,[11] and multiple exciton generation,[12] offering promise for next-generation optoelectronic devices.

In many nanocrystal syntheses the chemical reaction between nanocrystal precursors slowly releases soluble monomers, leading to supersaturation, nucleation, and growth (Scheme 1).[13,14] Monomer supply often limits the rate of the crystallization process, thereby influencing nanocrystal size, shape, and composition.[4,15–21] As a result, by manipulating the precursor reaction one can adjust the monomer supply kinetics and subsequent crystallization steps to produce a desired shape and size. Reproducible reaction kinetics are therefore key to predictable control over nanocrystal syntheses. Toward this end, recent efforts have elucidated the mechanism of several precursor reactions.[16,22–25] In particular, the reaction between tertiary phosphine chalcogenides and cadmium carboxylate or phosphonate complexes has been studied by several groups, leading to the conclusion that Lewis-acid

* Address correspondence to jso2115@columbia.edu.

Received for review August 17, 2012 and accepted October 8, 2012.

Published online October 08, 2012
10.1021/nn303769h

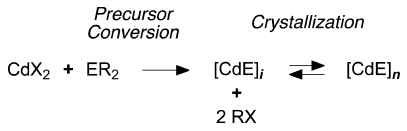

Scheme 1. Precursor conversion leads to soluble monomers that undergo crystallization.

activation leads to cleavage of the phosphorus–chalcogen bond.[22,23,25] Secondary phosphine chalcogenide reactivity is more complex and has been the subject of recent investigations,[18,26] particularly in the synthesis of lead chalcogenides, where the tertiary phosphine chalcogenide precursors undergo sluggish conversion,[24,27,28] and in the low-temperature formation of clusters.[24,29] These low-temperature studies report the *in situ* conversion of diphenylphosphine selenide to diphenyldiselenophosphinate derivatives that were characterized by single-crystal X-ray diffraction as a complex of lead[24] or using NMR spectroscopy.[29]

In an effort to understand the chemistry of secondary phosphine chalcogenides in nanocrystal syntheses, we have investigated the conversion of cadmium bis(diphenyldithiophosphinate) ($Cd(S_2PPh_2)_2$) to cadmium sulfide nanocrystals. Metal bis(dichalcogenidophosphinate) complexes are well-known[30−37] and have been used as single-source precursors for II–VI nanocrystals[37,38] and semiconductor thin films;[39] however the details of their reactivity in solution have not been explored in depth. Herein we explore the reaction of $Cd(S_2PPh_2)_2$ with cadmium tetradecanoate and demonstrate that it provides a facile and reliable synthesis of CdS nanocrystals with a narrow size distribution. We demonstrate that cadmium tetradecanoate activates the dithiophosphinate complex, leading to tetradecanoic anhydride and cadmium bis(diphenylphosphinate) ($Cd(O_2PPh_2)_2$)—products analogous to those resulting from conversion of tertiary phosphine chalcogenide precursors.[22,23] With an understanding of the reaction chemistry in hand, we optimize a synthesis that leads to complete conversion of the molecular precursors and show that the precursor reaction limits the rate of the crystallization.

RESULTS AND DISCUSSION

$Cd(S_2PPh_2)_2$ is readily synthesized in high yield and on large scale from tri*n*-butylammonium diphenyldithiophosphinate ($[Bu_3NH]^+[S_2PPh_2]^-$) and cadmium carboxylate according to Scheme 2. $[Bu_3NH]^+[S_2PPh_2]^-$ is conveniently obtained in a single-step reaction from diphenylphosphine, tri-*n*-butylamine, and elemental sulfur at room temperature. Solutions of $[Bu_3NH]^+[S_2PPh_2]^-$ in acetonitrile react with anhydrous cadmium benzoate or cadmium acetate, producing the corresponding tri-*n*-butylammonium carboxylate and causing precipitation of $Cd(S_2PPh_2)_2$,[31,32,37] which is polymeric in the solid state and insoluble in common solvents.[40] However, Lewis bases, such as primary alkylamines or tetramethylethylene diamine (TMEDA), bind the cadmium center and produce soluble complexes that can be used to grow single crystals suitable for X-ray crystallography (see Figure 1 and Table S1). Coordination of *n*-octylamine to $Cd(S_2PPh_2)_2$ is visible in the ^{31}P NMR spectrum, which displays a single resonance (δ = 64.0 ppm, 2 equiv of *n*-octylamine in C_6D_6) that shifts upfield to δ = 62.5 ppm as the concentration of added *n*-octylamine increases (Figure S2). The gradual change in chemical shift results from the dynamic equilibrium between ligated and unligated species that rapidly interconvert on the NMR time scale, behavior typical of ligand substitution at cadmium centers.[41]

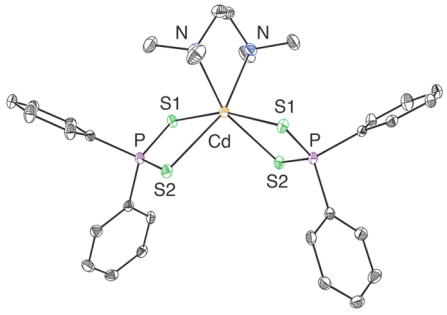

Figure 1. Molecular structure of TMEDA-coordinated Cd-$(S_2PPh_2)_2$ complex. Selected bond lengths (Å): Cd–S(1) 2.7482(7), Cd–S(2) 2.7015(7), P–S(1) 1.9960(9), P–S(2) 1.9974(9), Cd–N 2.421(2).

Heating $Cd(S_2PPh_2)_2$ to 240 °C in a high-boiling solvent does not produce CdS nanocrystals, indicating that it is not an effective single-source precursor under these conditions. However, when heated with cadmium tetradecanoate, nanocrystals with narrow absorption features and bright photoluminescence

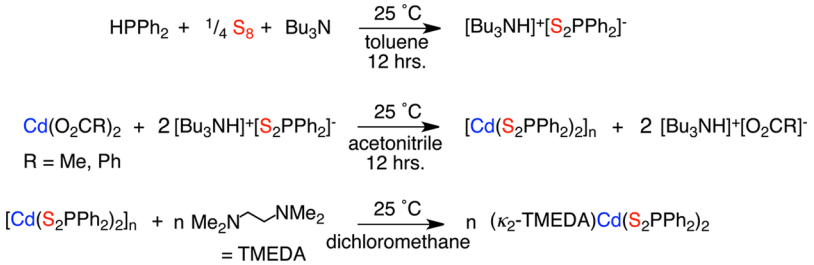

Scheme 2. Synthesis of cadmium bis(diphenyldithiophosphinate) complexes.

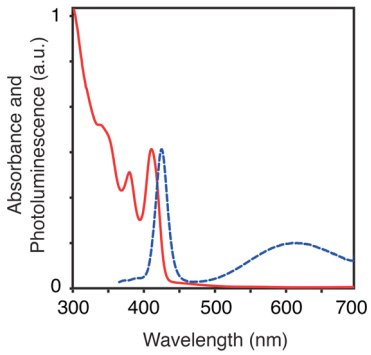

Figure 2. Representative absorption (red) and photoluminescence (blue dashed) spectra of crude CdS nanocrystals prepared from $Cd(S_2PPh_2)_2$ and cadmium tetradecanoate.

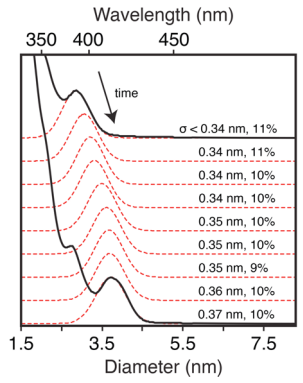

Figure 3. Gaussian functions (red, dashed) representing the distribution of nanocrystal diameters in aliquots removed during a reaction. The Gaussians were obtained by fitting histograms of nanocrystal diameters (black, solid) extracted from the absorbance spectra. Nanocrystals with similar size distributions are shown in Figures 2 and 6. Homogenous line broadening of individual nanocrystals is ignored in this analysis, implying that σ and $\%\sigma$ are overestimates of the actual polydispersity of the sample.

appear, as evidenced by spectra of the crude reaction mixture shown in Figure 2 ($PLQY_{band\ \ edge+trap} = 36\%$). The lowest energy absorption maximum of the nanocrystals invariably falls between 412 and 422 nm, corresponding to an average diameter of 3.8−4.1 nm according to the sizing formula published by Yu *et al.*[42] High-resolution transmission electron micrographs suggest a significantly smaller diameter of ∼3.5 nm (Figure S3). The line width of the first electronic transition from a typical synthesis has a full width at half-maximum height (fwhm) of 0.17 eV or less, corresponding to a standard deviation of less than 10% and among the narrowest distributions reported for colloidal CdS.[43−46] Powder X-ray diffraction of isolated nanocrystals is consistent with a predominantly zinc blende phase (Figure S4).

Figure 2 shows the sharp band-edge photoluminescence (fwhm = 0.11 eV) offset from the absorbance maximum by a 0.06 eV Stokes shift, as well as a broad trap emission centered at ∼630 nm, which is a common feature of CdS nanocrystal photoluminescence.[16,43−45] Taking into account both emission features the total photoluminescence quantum yield is as high as 36% when compared with a coumarin-153 standard.[47] Most reports of PLQY for colloidal CdS are ≤12%;[43,44] however there are reports as high as 30%[46] and 46%.[45] Over the course of the reaction a "photoluminescence bright point" is observed that is strongly correlated with the initial cadmium to sulfur ratio, much like what has been observed previously[48] (Figure S5). At all Cd:S ratios the photoluminescence peaks <10 min into the reaction, followed by a subsequent decrease. However, at a high cadmium to sulfur ratio (2:1) the quantum yield does not significantly decay, maintaining a $PLQY_{band\ edge+trap}$ of >30% over the duration of the reaction.

Monitoring the crystallization by removing aliquots during growth shows a decrease in the breadth of the lowest energy electronic absorption (σ_{fwhm} = 0.09 → 0.07 eV). Extracting a diameter distribution from the absorption spectrum reveals that the spectral narrowing observed here corresponds to a slight *increase* in the absolute size distribution (Figure 3; σ = 0.34 → 0.37 nm). Although size focusing is not observed, Ostwald ripening is slow under these conditions, even when the reaction is heated much longer than the time required to convert all nanocrystal precursors. However, size distribution broadening does occur when reactions are run in the presence of added oleic acid, in agreement with previous studies that show acidic surfactants catalyze Ostwald ripening.[15] Thus, it appears that the absence of free acids in this synthesis is at least partially responsible for the narrow size distributions obtained.

Unlike most II−VI nanocrystal syntheses, the final size is relatively *insensitive* to changes in the reaction conditions. Nanocrystals consistently form with a first electronic absorption maximum at 412−422 nm and comparable line width despite changes to the chain length of the carboxylate (undecanoate *vs* tetradecanoate), the ratio of Cd:S (2:1 *vs* 4:1), the reaction solvent (hexadecane *vs* 1-octadecene), reaction time (40 min *vs* 120 min), or total concentration (1−5×) (Figure S6). This invariance to reaction conditions and slow Ostwald ripening make the size of nanocrystals obtained using this method highly reproducible; a hypothesis for this phenomenon is discussed below. Larger nanocrystals with narrow size distributions can be synthesized if additional precursors are added (as solids) to a standard synthesis that has reached completion, which leads to nanocrystal growth and not formation of new nuclei. As shown in Figure 4, this provides access to nanocrystals ranging in diameter from 3.9 to 5.4 nm.[42] By tuning the amount of precursors added, the desired size of nanocrystals can be achieved in full yield.

To gain insight into the mechanism of the precursor conversion, the reaction co-products were identified.

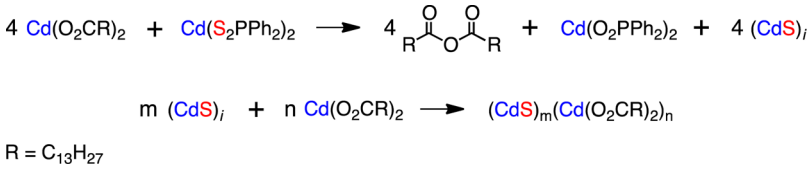

Scheme 3. Balanced chemical equation for the conversion of cadmium bis(diphenyldithiophosphinate) to cadmium sulfide nanocrystals.

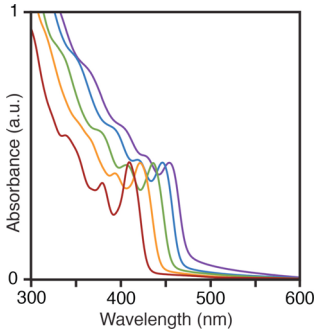

Figure 4. Absorbance spectra of larger nanocrystals grown by adding additional precursors (as solids) to a standard synthesis that has reached completion.

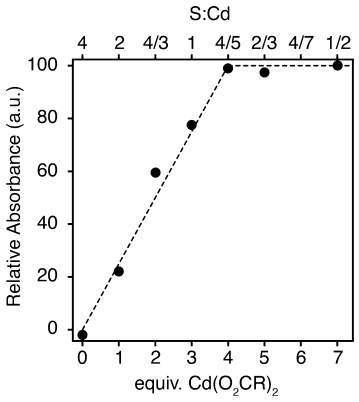

Figure 5. Relative absorbance of completed reactions that were initiated with varying amounts of cadmium tetradecoate ($Cd(O_2CR)_2$). The dashed line assumes the balanced chemical reaction in Scheme 2.

Much like the $Cd(S_2PPh_2)_2$ precursor, the crude product mixture is partially insoluble in d_6-benzene and shows little to no ^{31}P NMR signal. Adding a Lewis base (*e.g.*, octylamine) produces a clear yellow solution with a single, sharp ^{31}P NMR resonance (δ = 19.2 ppm). This phosphorus-containing co-product is assigned as cadmium bis(diphenylphosphinate) ($Cd(O_2PPh_2)_2$) by comparison of its spectrum with an independently synthesized sample (Figure S7). Like $Cd(S_2PPh_2)_2$, $Cd(O_2PPh_2)_2$ is an insoluble coordination polymer unless Lewis-basic ligands are present, which has been observed previously for this and other cadmium phosphinate complexes.[49,50] Infrared spectroscopy of the crude reaction mixture also shows a diagnostic signal for tetradecanoic anhydride (ν = 1755, 1820 cm^{-1}), the assignment of which was verified by comparison with a commercial sample (Figure S8). Isolated nanocrystals were analyzed with ^1H NMR spectroscopy and showed signals consistent with tetradecanoate termination. The ligands were further analyzed by cleaving them from the nanocrystal with trimethylsilyl chloride (Me_3Si-Cl), leading to insoluble chloride-terminated nanocrystals and trimethylsilyl esters of the ligands.[51] ^{13}C, ^1H, and ^{31}P NMR of the soluble byproducts demonstrated exclusive formation of trimethylsilyltetradecanoate, confirming that the nanocrystals are bound solely by tetradecanoate ligands (no signatures of trimethylsilyldiphenylphosphinate are visible; see Figures S9 and S10).

On the basis of the co-product assignments we propose a balanced reaction for this transformation where $Cd(S_2PPh_2)_2$ deoxygenates cadmium tetradecanoate, leading to tetradecanoic anhydride and $Cd(O_2PPh_2)_2$ (Scheme 3).[52] The proposed stoichiometry is further supported by comparing the initial ratio of cadmium tetradecanoate and $Cd(S_2PPh_2)_2$ with the final yield of CdS. Figure 5 shows that the relative absorbance of CdS increases as the amount of cadmium tetradecanoate is increased, reaching a plateau at 5:4 cadmium:sulfur due to the cadmium-containing co-product in the proposed stoichiometry. ^{31}P NMR spectroscopy of the reaction mixture also corroborates the proposed stoichiometry, demonstrating complete conversion of the dithiophosphinate precursor to the phosphinate co-product at this Cd:S ratio ($\geq$5:4; Figure 6). Together, these results imply that all sulfur atoms in $Cd(S_2PPh_2)_2$ are converted to cadmium sulfide in the presence of $\geq$4 equivalents of cadmium tetradecanoate. Additional equivalents of cadmium tetradecanoate are needed to passivate the nanocrystal surface;[53] a standard synthesis utilizes seven equivalences of cadmium tetradecanoate (3 excess) in order to maintain maximum photoluminescence for the duration of the reaction as described above.

The co-products described above are analogous to those produced from the reaction of tertiary or secondary phosphine chalcogenides with metal carboxylates, where a Lewis-acid activation mechanism results in a tertiary phosphine oxide and carboxylic acid anhydride.[22,23] A similar pathway appears to be important in the present case, particularly because $Cd(S_2PPh_2)_2$ does not undergo reaction in the absence of cadmium tetradecanoate. This pathway differs from previous work on secondary phosphine chalcogenides

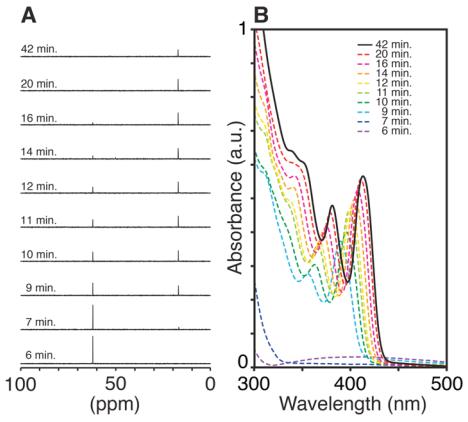

Figure 6. Time-dependent ^{31}P NMR spectra (left) and UV−visible absorbance spectra (right). The NMR shows conversion from the $Cd(S_2PPh_2)_2$ precursor to the $Cd(O_2PPh_2)_2$ co-product, enabling a measure of the precursor reaction. The absorbance spectra enable a measured nanocrystal formation. (Note: The $Cd(O_2PPh_2)_2$ peak slightly broadens with time, causing the height to decrease. The integrals of the initial and final peaks match.)

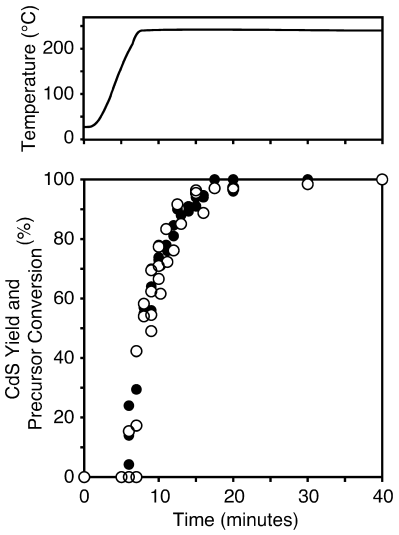

Figure 7. Summary of kinetics data showing both precursor conversion (filled circles) and nanocrystal formation (empty circles), determined from ^{31}P NMR and UV−vis absorbance spectroscopies, respectively. The data points, and thus reaction rates, correspond closely with one another. The panel above shows the temperature change during a typical reaction.

in which zerovalent lead is believed to be an intermediate[22,27] and conversion of $Cd(Se_2PPh_2)_2$ occurs at much lower temperature in the presence of additional diphenylphosphine.[29] Reaction with the solvent does not appear to be important because similar reaction rates were observed in 1-octadecene or a saturated hydrocarbon (hexadecane).[16]

Having identified the underlying precursor reaction stoichiometry, we investigated the relative rates of precursor conversion and nanocrystal formation with ^{31}P NMR and UV−visible absorption spectroscopies, respectively (Figure 6). Figure 7 shows the percentage of precursors converted and the percent yield of cadmium sulfide *versus* time. The strong correspondence between the rates of these processes indicates that the crystallization rate is limited by the precursor conversion kinetics and supports a nucleation and growth mechanism, much like has been observed in other nanocrystal syntheses.[15,17,54,55]

In our study the final number of nanocrystals is proportional to the initial precursor concentration. This follows from the invariability in the final size with respect to the total concentration, the quantitative conversion of $Cd(S_2PPh_2)_2$, and the lack of Ostwald ripening. Previous studies have made related observations and suggest that the number of nanocrystals depends on the rate of solute formation during nucleation.[15,17] In that work the precursor conversion rate and the number of nanocrystals display a second-order concentration dependence. In contrast, under our conditions the final number of nanocrystals is directly proportional to changes in the precursor concentration over a factor of 5; that is, nucleation has a first-order dependence on total precursor concentration. Combined with reproducible conversion chemistry this first-order concentration dependence is likely responsible for the invariability in the final size.

The reactivity described above has significant implications for nanocrystal syntheses that utilize single-source precursors or secondary phosphine chalcogenides. In particular, Lewis-acid activation of the dithiophosphinate is likely an important step to monomer generation, suggesting that other "single-source" precursors may undergo more facile conversion to nanocrystals in the presence of added metal carboxylate or phosphonate salts. Furthermore, the rapid formation of dichalcogenidophosphinate derivatives from secondary phosphines and their complexation with cadmium and lead[24] may be an important parallel path to the reduction pathways proposed by others in secondary phosphine based reactions.[22,24,27]

CONCLUSION

We have identified a new synthetic route to CdS nanocrystals based on the reaction between cadmium bis(diphenyldithiophosphinate) and cadmium carboxylate. Nanocrystals formed under these conditions consistently fall within a narrow range of sizes and exhibit unusually sharp absorption features. This behavior results from well-defined and reproducible precursor reactivity and a lack of Ostwald ripening. Unambiguous characterization of the tetradecanoic anhydride and $Cd(O_2PPh_2)_2$ co-products allows us to write a balanced chemical equation for the precursor reaction (Scheme 3). With this knowledge we were able to optimize a synthesis that provides cadmium sulfide nanocrystals in quantitative yield and obtain

nanocrystals with unambiguous chemical composition. The observed co-products are analogous to those resulting from tertiary phosphine chalcogenide precursors, suggesting a similar Lewis-acid activation pathway is likely important in this case. From this we suggest that Lewis-acidic metal complexes could activate related single-source precursors, significantly improving their utility in nanocrystal syntheses. In addition to their consistent size and narrow size distribution, their bright photoluminescence ($PLQY_{band\ \ edge+trap}$ = 36%) and unambiguous chemical composition make these nanocrystals ideal candidates for studying nanocrystal chemistry.

EXPERIMENTAL SECTION

Materials and Methods. All manipulations were performed under air-free conditions unless otherwise indicated using standard Schlenk techniques and/or in a nitrogen-filled glovebox. Cadmium nitrate tetrahydrate (99%), sodium hydroxide, tetradecanoic acid (99%), undecanoic acid (98%), diphenylphosphinic acid (98%), methanol (99.8%), benzoic acid (>99.5%), tetradecanoic anhydride (95%), coumarin 153, hexadecane (99%), and 1-octadecene (90%) were obtained from Sigma Aldrich and used without further purification. Tri-*n*-butylamine (99%), *n*-octylamine (99%), and chlorotrimethylsilane (99%) were obtained from Sigma Aldrich; tetramethylethylenediamine (99%) was obtained from Strem Chemicals; all were dried over CaH_2, distilled, and stored under nitrogen prior to use. Diphenylphosphine (99%) was obtained from Strem and used without further purification. $CdMe_2$ was purchased from Strem and vacuum distilled prior to use. *CAUTION: Dimethylcadmium is an extremely toxic liquid and due to its volatility and air-sensitivity should only be handled by a highly trained and skilled scientist.* Cadmium tetradecanoate and cadmium undecanoate were prepared on a 5 mmol scale according to Chen *et al*.[56] Pentane (99%) and toluene (99%) were dried over alumina drying columns, shaken with activated alumina, and stored over 4 Å molecular sieves for at least 24 h prior to use. Benzene-d_6 (99.6%), anhydrous acetonitrile (99.8%), and anhydrous methyl acetate (99.5%) were purchased from Sigma Aldrich, shaken with activated alumina, filtered, and stored over 4 Å molecular sieves for at least 24 h prior to use. ACS grade toluene (>99.5%) used for optical spectroscopy was purchased from Sigma Aldrich and used without further purification. CD_2Cl_2 was purchased from Cambridge Isotope Laboratories, filtered over activated alumina, and stored over 4 Å molecular sieves for at least 24 h prior to use.

NMR spectra were recorded on Bruker Avance III 400 and 500 MHz instruments. UV−visible absorption data were obtained using a Perkin-Elmer Lamda 650 spectrophotometer equipped with deuterium and tungsten halogen lamps. Fluorescence measurements were performed using a FluoroMax 4 from Horiba Scientific. FT-IR spectra were obtained on a Thermo Scientific Nicolet 6700 spectrometer equipped with a liquid N_2 cooled MCT-A detector. Powder XRD analysis was performed on an Inel X-ray diffractometer equipped with a wide-angle detector. Quantum yield was measured against a freshly prepared coumarin standard in ethanol (PLQY = 53%) by exciting at the point where the absorption of the CdS and coumarin overlapped (~390 nm) and taking into account the different indices of refraction of the solvents according to Kuznetsova.[47] ^{31}P NMR spectra were externally referenced to 85% H_3PO_4 at 0 ppm.

Synthesis of $Cd(O_2P(C_6H_5)_2)_2$ (cadmium diphenylphosphinate). Following a procedure analogous to that used to make cadmium tetradecanoate,[56] 1 equivalent of cadmium nitrate tetrahydrate (0.15 g; 0.5 mmol) was dissolved in 5 mL of methanol. Sodium diphenylphosphinate was prepared by mixing 3 equivalents of sodium hydroxide (0.06 g; 1.5 mmol) and 3 equivalents of diphenylphosphinic acid (0.33 g; 1.5 mmol) in 50 mL of methanol. The cadmium nitrate solution was then added to the diphenylphosphinate solution dropwise over 10 min with vigorous stirring. Following 1 h of stirring ~80% of the methanol was removed by rotary evaporation, and the resulting white powder was isolated *via* filtration. The powder was washed three times with methanol and dried under vacuum at ~60 °C overnight (0.25 g; 90%). The isolated powder was insoluble in common organic solvents; however solutions for NMR spectroscopy can be obtained by adding TMEDA. ^1H NMR (CD_2Cl_2, 500 MHz): δ 2.18 (s, TMEDA, $-CH_3$), 2.32 (s, TMEDA, $-CH_2$), 7.19 (b, 2H, *m*-CH), 7.30 (b, 1H, *p*-CH), 7.65 (b, 2H, *o*-CH). $^{13}C\{^1H\}$ NMR (CD_2Cl_2, 125.7 MHz): δ 46.18 (s, TMEDA, $-CH_3$), 58.25 (s, TMEDA, $-CH_2$), 127.69 (b, 2H, *m*-C), 129.80 (b, 1H, *p*-C), 131.29 (b, 2H, *o*-C). $^{31}P\{^1H\}$ NMR (CD_2Cl_2, 202.4 MHz): δ 22.90 (s).

Synthesis of $Cd(O_2CC_6H_5)_2$ (cadmium benzoate). This procedure is similar to previous examples of using dimethylcadmium to prepare cadmium salts.[51] In a nitrogen-filled glovebox, benzoic acid (6.84 g; 56 mmol) was suspended in a mixture of pentane (120 mL) and toluene (20 mL), and the vessel wrapped in aluminum foil. With the lights turned off, dimethylcadmium (3.99 g; 28 mmol) was added dropwise to the suspension over 10 min, causing bubbling of the solution. The resulting white slurry was stirred for 3 h in the dark, and the resulting precipitate was isolated by filtration, washed with pentane, and dried to a constant mass under vacuum (9.54 g, 96%). The isolated powder is insoluble in common organic solvents. Solutions for NMR spectroscopy were obtained by adding an excess of TMEDA. ^1H NMR (CD_2Cl_2, 500 MHz): δ 2.24 (s, TMEDA, $-CH_3$), 2.38 (s, TMEDA, $-CH_2$), 7.37 (t, 2H, *m*-CH), 7.45 (t, 1H, *p*-CH), 8.06 (d, 2H, *o*-CH). $^{13}C\{^1H\}$ NMR (CD_2Cl_2, 125.7 MHz): δ 46.30 (s, TMEDA, $-CH_3$), 58.11 (s, TMEDA, $-CH_2$), 128.31 (*b*, *m*-C), 130.63 (*b*, *o*-C), 131.51 (*b*, *p*-C), 175.35 (s, 1-C).

Synthesis of $[Bu_3NH]^+[S_2PPh_2]^-$. To a round-bottom flask equipped with a stir bar, sulfur powder (960 mg; 30 mmol), diphenylphosphine (2.79 g; 15 mmol), and tri-*n*-butylamine (2.78 g; 15 mmol) were added to 35 mL of toluene at room temperature, and the mixture was left stirring overnight. The solvent was removed *in vacuo*, leaving an oily residue, which was triturated with pentane (20 mL), filtered, and washed with additional pentane (50 mL). The resulting white powder was dried under vacuum (6.21 g; 95%). $[Bu_3NH]^+[S_2PPh_2]^-$ can be stored indefinitely at room temperature under an inert atmosphere. Slow evaporation of a diethyl ether solution produced single crystals of $[Bu_3NH]^+[S_2PPh_2]^-$ suitable for X-ray crystallography (see Table S1 for structure parameters and Figure S12 for an ORTEP diagram). ^1H NMR (CD_2Cl_2, 500 MHz): δ 0.87 (t, 3H, CH_3), 1.29 (m, 2H, CH_2), 1.66 (m, 2H, CH_2), 3.07 (m, 2H, CH_2), 7.30 (m, 3H, *m*-CH and *p*-CH), 8.08 (m, 2H, *o*-CH), 10.02 (b, 1H, NH). $^{13}C\{^1H\}$ NMR (CD_2Cl_2, 125.7 MHz): δ 13.89 (s, CH_3), 20.55 (s, CH_2), 25.43 (s, CH_2), 52.25 (s, CH_2), 127.90 (d, *m*-C), 129.54 (d, *p*-C), 131.02 (d, *o*-C). $^{31}P\{^1H\}$ NMR (CD_2Cl_2, 202.4 MHz): δ 60.86 (s).

Synthesis of $Cd(S_2PPh_2)_2$ (cadmium bis(diphenyldithiophosphinate)). Following a variation on previous syntheses utilizing metal halide salts and ammonium dithiophosphinates,[31,32,37] $[Bu_3NH]^+[S_2PPh_2]^-$ (2.61 g; 6 mmol), cadmium benzoate (1.06 g; 3 mmol), and acetonitrile (100 mL) were added to a 250 mL round-bottom flask equipped with a stir bar. The solution was left stirring overnight, resulting in a pale pink suspension. The acetonitrile was removed *in vacuo*, leaving an oily residue, to which methyl acetate (5 mL) was added. Pentane (~8 mL) was then added, the mixture filtered through a glass frit, and the white powder washed twice with pentane (50 mL) and dried under vacuum (1.47 g; 80%). The complex was unchanged when stored under ambient conditions after >6 months, as confirmed by NMR spectroscopy. The complex is insoluble in common organic solvents;[57] however it is minutely soluble in dichloromethane-d_2 such that a ^{31}P NMR spectrum could be obtained, matching that of a previously reported synthesis of this compound.[33] ^1H NMR (CD_2Cl_2, 500 MHz): δ 7.49 (m, 3H, *m*-CH and *p*-CH), 7.97 (m, 2H, *o*-CH). $^{31}P\{^1H\}$ NMR (CD_2Cl_2, 161.9 MHz): δ 65.7 (s).

Synthesis of $Cd(S_2PPh_2)_2$(TMEDA). Excess tetramethylethylenediamine was added to a suspension of $Cd(S_2PPh_2)_2$ in dichloromethane, resulting in a clear and colorless solution. Slow evaporation of the solvent produced single crystals of $Cd(S_2PPh_2)_2$(TMEDA) suitable for X-ray crystallography (see Table S1 for structure parameters and Figure 1 for an ORTEP diagram). ^{1}H NMR (CD_2Cl_2, 500 MHz): δ 2.19 (s, TMEDA, $-CH_3$), 2.35 (s, TMEDA, $-CH_2$), 7.37 (b, 2H, *m*-CH), 7.42 (b, 1H, *p*-CH), 7.99 (b, 2H, *o*-CH). $^{13}C\{^1H\}$ NMR (CD_2Cl_2, 125.7 MHz): δ 46.08 (s, TMEDA, $-CH_3$), 58.11 (s, TMEDA, $-CH_2$), 127.80 (b, 2H, *m*-C), 130.01 (b, 1H, *p*-C), 130.76 (b, 2H, *o*-C). $^{31}P\{^1H\}$ NMR (CD_2Cl_2, 202.4 MHz): δ 64.01 (s).

Synthesis of CdS Nanocrystals. $Cd(S_2PPh_2)_2$ (15.3 mg; 0.025 mmol) and cadmium tetradecanoate (99.3 mg; 0.175 mmol) were added to a three-neck round-bottom flask fitted with a septum, distillation head, and glass thermocouple probe adapter. 1-Octadecene was added (6.3 mL), and the mixture was degassed (<50 mbar) with vigorous stirring for 1 h, after which the reaction vessel was filled with argon. The solution was then heated to 240 °C at an average rate of 40 °C min^{-1} using a heating mantle and temperature controller. Timing began when the mantle was turned on, and beginning at t = 6 min, 25 μL aliquots were removed and dissolved in 2.5 mL of toluene in air and UV–vis and fluorescence measurements were acquired. At the completion of the reaction (normally 40 min) the reaction vessel was cooled to ~100 °C.

Isolation of CdS Nanocrystals. Upon cooling to 100 °C, volatiles were removed by distillation under vacuum (20–50 mbar). The resultant residue was dissolved in toluene (2 mL), TMEDA (0.5 mL) was added, and the suspension was centrifuged at 7000 rpm for 10 min. The translucent golden solution was decanted, and the pellet discarded. Acetonitrile was added until the solution maintained cloudiness upon mixing, which was followed by an extra ~0.5 mL added, after which the solids were isolated by centrifugation. The yellow precipitate was redissolved in toluene and TMEDA and precipitated by adding acetonitrile a second time. The resultant yellow precipitate was then dissolved in toluene only (without TMEDA) and precipitated with acetonitrile. This previous step was repeated twice more, the resultant pale yellow powder dissolved in pentane and centrifuged a final time to remove insoluble material, and the pale yellow solution containing the nanocrystals was decanted.

Ligand Characterization. A sample of isolated nanocrystals was dissolved in anhydrous C_6D_6, to which an excess of Me_3Si-Cl was added under nitrogen. Upon addition of the Me_3Si-Cl, the nanocrystals precipitated. The sample was allowed to react for at least 15 min, after which it was characterized by ^{1}H, ^{13}C, and ^{31}P NMR spectroscopies. The trimethylsilyltetradecanoate is assigned as follows: ^{1}H NMR (C_6D_6, 500 MHz): δ 0.21 (s, $-Si(CH_3)_3$), 0.90 (t, 3H, $-CH_3$), 1.20–1.30 (b, 20H, $-CH_2$), 1.56 (m, 2H, β-CH_2), 2.18 (b, 2H, α-CH_2). $^{13}C\{^1H\}$ NMR (CD_2Cl_2, 125.7 MHz): δ 0.11 (s, $-Si(CH_3)_3$), 2.12 (s, $-Si(CH_3)_3$), 3.12 (s, $-Si(CH_3)_3$), 14.40 (s, $-CH_3$), 23.15 (s, $-CH_2$), 25.41 (s, $-CH_2$), 29.47 (s, $-CH_2$), 29.51 (s, $-CH_2$), 29.76 (s, $-CH_2$), 29.86 (s, $-CH_2$), 29.96 (s, $-CH_2$), 30.09 (s, $-CH_2$), 30.15 (b, $-CH_2$), 30.18 (s, $-CH_2$), 32.39 (s, $-CH_2$), 36.08 (s, α-CH_2), 173.65 (s, $-C(O)O$).

Kinetics. The procedure for nanocrystal synthesis described above was carried out at twice the scale. Aliquots (250 μL) were taken with a glass microliter syringe at 1 min intervals starting at t = 5 min. A portion of this aliquot (200 μL) was added to an NMR tube containing C_6D_6 (300 μL) and octylamine (100 μL) and used to monitor the ratio of the dithiophosphinate precursor and phosphinate product. No other intermediates were visible in the ^{31}P NMR spectra. The remainder of the aliquot (50 μL) was added to 2.5 mL of toluene for analysis with UV–visible absorbance spectroscopy. The percent conversion was measured by comparing the relative integrals of the ^{31}P NMR signals from $Cd(O_2PPh_2)_2$ and $Cd(S_2PPh_2)_2$. No mixed O/S intermediates are visible. Relative CdS yield was determined by comparing the concentration of CdS at each time point with the concentration of CdS at full conversion. The concentration of CdS was estimated from the product of the nanocrystal concentration and nanocrystal molar volume as determined from the absorbance and wavelength of the lowest energy absorption maximum according to Yu *et al.*[42] Estimating the percent yield relative to the known end point of 100% reduces the impact of systematic error in the extinction coefficient of CdS.

Size Distribution Analysis. Each point in the absorption spectra was converted from wavelength to diameter and corrected for the size-dependent extinction according to Yu *et al.*[42] The region corresponding to the lowest energy absorption in the transformed spectra (now a histogram of diameters) was fit with a Gaussian function using a least-squares analysis. Values of diameters beyond the first excitonic transition are meaningless and were not included in the fit. The center of the Gaussian corresponds to the average size of the nanocrystals and the breadth of the Gaussian to the polydispersity of the sample. The standard deviation (σ) was extracted and used to calculate the percent standard deviation (%σ) by dividing σ by the average diameter. Homogenous line broadening of individual nanocrystals is ignored in this analysis, resulting in σ and %σ that are slight overestimates (~25%) of the actual polydispersity of the sample.[58]

Conflict of Interest: The authors declare no competing financial interest.

Acknowledgment. The authors acknowledge the National Science Foundation through contract number NSF-CHE-1151172 for funding. C. Cunningham and A. Wolcott are acknowledged for help with TEM, some of which was carried out at the Center for Functional Nanomaterials, Brookhaven National Laboratory, which is supported by the U.S. Department of Energy, Office of Basic Energy Sciences, under Contract No. DE-AC02-98CH10886. We thank A. Kreider-Mueller, N. Chakrabarti, and G. Parkin for crystal structure determination and the National Science Foundation (CHE-0619638) for acquisition of an X-ray diffractometer.

Supporting Information Available: X-ray crystal structure parameters, NMR spectra of amine complexes of $Cd(S_2PPh_2)_2$, transmission electron micrographs, powder X-ray diffraction, photoluminescence data, UV–visible absorbance spectra demonstrating insensitivity to reaction conditions, NMR and FT-IR spectra used for co-product identification, NMR spectra used for ligand identification, and an ORTEP diagram of $[Bu_3NH]^+$-$[S_2PPh_2]^-$ are provided. This material is available free of charge *via* the Internet at http://pubs.acs.org.

REFERENCES AND NOTES

1. Burda, C.; Chen, X.; Narayanan, R.; El-Sayed, M. A. Chemistry and Properties of Nanocrystals of Different Shapes. *Chem. Rev.* **2005**, *105*, 1025–1102.
2. Schliehe, C.; Juarez, B. H.; Pelletier, M.; Jander, S.; Greshnykh, D.; Nagel, M.; Meyer, A.; Foerster, S.; Kornowski, A.; Klinke, C.; *et al.* Ultrathin PbS Sheets by Two-Dimensional Oriented Attachment. *Science* **2010**, *329*, 550–553.
3. Ithurria, S.; Bousquet, G.; Dubertret, B. Continuous Transition from 3D to 1D Confinement Observed during the Formation of CdSe Nanoplatelets. *J. Am. Chem. Soc.* **2011**, *133*, 3070–3077.
4. Ruberu, T. P. A.; Albright, H. R.; Callis, B.; Ward, B.; Cisneros, J.; Fan, H.-J.; Vela, J. Molecular Control of the Nanoscale: Effect of Phosphine-Chalcogenide Reactivity on CdS-CdSe Nanocrystal Composition and Morphology. *ACS Nano* **2012**, *6*, 5348–5359.
5. Reiss, P.; Protiere, M.; Li, L. Core/Shell Semiconductor Nanocrystals. *Small* **2009**, *5*, 154–168.
6. Carbone, L.; Nobile, C.; De Giorgi, M.; Sala, F. D.; Morello, G.; Pompa, P.; Hytch, M.; Snoeck, E.; Fiore, A.; Franchini, I. R.; *et al.* Synthesis and Micrometer-Scale Assembly of Colloidal CdSe/CdS Nanorods Prepared by a Seeded Growth Approach. *ACS Nano* **2007**, *7*, 2942–2950.
7. Talapin, D. V.; Nelson, J. H.; Shevchenko, E. V.; Aloni, S.; Sadtler, B.; Alivisatos, A. P. Seeded Growth of Highly Luminescent CdSe/CdS Nanoheterostructures with Rod and Tetrapod Morphologies. *ACS Nano* **2007**, *7*, 2951–2959.
8. Norris, D. J.; Efros, A. L.; Erwin, S. C. Doped Nanocrystals. *Science* **2008**, *319*, 1776–1779.

9. Chen, Y.; Vela, J.; Htoon, H.; Casson, J. L.; Werder, D. J.; Bussian, D. A.; Klimov, V. I.; Hollingsworth, J. A. "Giant" Multishell CdSe Nanocrystal Quantum Dots with Suppressed Blinking. *J. Am. Chem. Soc.* **2008**, *130*, 5026.
10. Wang, X.; Ren, X.; Kahen, K.; Hahn, M. A.; Rajeswaran, M.; Maccagnano-Zacher, S.; Silcox, J.; Cragg, G. E.; Efros, A. L.; Krauss, T. D. Non-Blinking Semiconductor Nanocrystals. *Nat. Mater.* **2009**, *459*, 686–689.
11. Yang, J.; Hyun, B.-R.; Basile, A. J.; Wise, F. W. Exciton Relaxation in PbSe Nanorods. *ACS Nano* **2012**, 8120–8127.
12. Cunningham, P. D.; Boercker, J. E.; Foos, E. E.; Lumb, M. P.; Smith, A. R.; Tischler, J. G.; Melinger, J. S. Enhanced Multiple Exciton Generation in Quasi-One-Dimensional Semiconductors. *ACS Nano* **2011**, *11*, 3476–3481.
13. LaMer, V. K.; Dinegar, R. H. Theory, Production and Mechanism of Formation of Monodispersed Hydrosols. *J. Am. Chem. Soc.* **1950**, *72*, 4847–4854.
14. Sugimoto, T. Preparation of Monodispersed Colloidal Particles. *Adv. Colloid Interface* **1987**, *28*, 65–108.
15. Owen, J. S.; Chan, E. M.; Liu, H.; Alivisatos, A. P. Precursor Conversion Kinetics and the Nucleation of Cadmium Selenide Nanocrystals. *J. Am. Chem. Soc.* **2010**, *132*, 18206–18213.
16. Li, Z.; Ji, Y.; Xie, R.; Grisham, S.; Peng, X. Correlation of CdS Nanocrystal Formation with Elemental Sulfur Activation and Its Implication in Synthetic Development. *J. Am. Chem. Soc.* **2011**, 17248–17256.
17. Abe, S.; Čapek, R. K.; De Geyter, B.; Hens, Z. Tuning the Postfocused Size of Colloidal Nanocrystals by the Reaction Rate: From Theory to Application. *ACS Nano* **2012**, *6*, 42–53.
18. Wang, F.; Buhro, W. Morphology Control of Cadmium Selenide Nanocrystals: Insights into the Roles of Di-*n*-octylphosphine Oxide (DOPO) and Di-*n*-octylphosphinic Acid (DOPA). *J. Am. Chem. Soc.* **2012**, 5369–5380.
19. Sugimoto, T.; Shiba, F. Spontaneous Nucleation Of Monodisperse Silver Halide Particles from Homogeneous Gelatin Solution II: Silver Bromide. *Colloid Surf., A* **2000**, *164*, 205–215.
20. Sugimoto, T.; Shiba, F.; Sekiguchi, T.; Itoh, H. Spontaneous Nucleation of Monodisperse Silver Halide Particles from Homogeneous Gelatin Solution I: Silver Chloride. *Colloid Surf., A* **2000**, *164*, 183–203.
21. Ghosh, Y.; Mangum, B. D.; Casson, J. L.; Williams, D. J.; Htoon, H.; Hollingsworth, J. A. New Insights into the Complexities of Shell Growth and the Strong Influence of Particle Volume in Nonblinking "Giant" Core/Shell Nanocrystal Quantum Dots. *J. Am. Chem. Soc.* **2012**, *134*, 9634–9643.
22. Steckel, J. S.; Yen, B. K. H.; Oertel, D. C.; Bawendi, M. G. On the Mechanism of Lead Chalcogenide Nanocrystal Formation. *J. Am. Chem. Soc.* **2006**, *128*, 13032–13033.
23. Liu, H.; Owen, J. S.; Alivisatos, A. P. Mechanistic Study of Precursor Evolution in Colloidal Group II–VI Semiconductor Nanocrystal Synthesis. *J. Am. Chem. Soc.* **2007**, *129*, 305–312.
24. Evans, C. M.; Evans, M. E.; Krauss, T. D. Mysteries of TOPSe Revealed: Insights into Quantum Dot Nucleation. *J. Am. Chem. Soc.* **2010**, *132*, 10973–10975.
25. Garcia-Rodriguez, R.; Liu, H. Mechanistic Study of the Synthesis of CdSe Nanocrystals: Release of Selenium. *J. Am. Chem. Soc.* **2012**, 1400–1403.
26. Yu, K.; Hrdina, A.; Zhang, X.; Ouyang, J.; Leek, D. M.; Wu, X.; Gong, M.; Wilkinson, D.; Li, C. Highly-Photoluminescent ZnSe Nanocrystals *via* a Non-Injection-Based Approach with Precursor Reactivity Elevated by a Secondary Phosphine. *Chem. Commun.* **2011**, *47*, 8811–8813.
27. Joo, J.; Pietryga, J. M.; McGuire, J. A.; Jeon, S.-H.; Williams, D. J.; Wang, H.-L.; Klimov, V. I. A Reduction Pathway in the Synthesis of PbSe Nanocrystal Quantum Dots. *J. Am. Chem. Soc.* **2009**, *131*, 10620–10628.
28. Yu, K.; Ouyang, J.; Leek, D. M. *In-Situ* Observation of Nucleation and Growth of PbSe Magic-Sized Nanoclusters and Regular Nanocrystals. *Small* **2011**, *7*, 2250–2262.
29. Cossairt, B. M.; Owen, J. S. CdSe Clusters: At the Interface of Small Molecules and Quantum Dots. *Chem. Mater.* **2011**, *23*, 3114–3119.
30. Lawton, S.; Kokotailo, G. Crystal and Molecular Structures of Zinc and Cadmium O,O-Diisopropylphosphorodithioates. *Inorg. Chem.* **1969**, 2410–2421.
31. Kuchen, W.; Hertel, H. Metal Complexes of Thiophosphinic and Selenophosphinic Acids. *Angew. Chem., Int. Ed.* **1969**, *8*, 89–97.
32. Cavell, R.; Day, E.; Byers, W.; Watkins, P. Metal Complexes of Substituted Dithiophosphinic Acids. V. Complexes of Manganese, Iron, and Cobalt. *Inorg. Chem.* **1972**, *11*, 1759–1772.
33. Annan, T. A.; Kumar, R.; Tuck, D. G. Direct Electrochemical Synthesis and Crystallographic Characterization of Metal Diphenylphosphido and Diphenylthiophosphinato Compounds, and Some Derivatives. *J. Chem. Soc. Dalton* **1991**, 11–18.
34. Haiduc, I.; Sowerby, D.; Shao-Fang, L. Stereochemical Aspects of Phosphor-1,1-dithiolato Metal Complexes: Coordination Patterns, Molecular Structures and Supramolecular Associations in Dithiophosphinates and Related Compounds. *Polyhedron* **1996**, *15*, 2469–2521.
35. Byrom, C.; Malik, M. A.; O'Brien, P.; White, A.; Williams, D. Synthesis and X-Ray Single Crystal Structures Of Bis-(diisobutyldithiophosphinato)cadmium(II) or Zinc(II): Potential Single-Source Precursors for II/VI Materials. *Polyhedron* **2000**, *19*, 211–215.
36. Nguyen, C.; Adeogun, A.; Afzaal, M.; Malik, M. A.; O'Brien, P. Metal Complexes of Selenophosphinates from Reactions with $(R_2PSe)_2Se$: $[M(R_2PSe_2)_n]$ (M= Zn^{II}, Cd^{II}, Pb^{II}, In^{III}, Ga^{III}, Cu^{I}, Bi^{III}, Ni^{II}; R= ^{i}Pr, Ph) and $[Mo^{V}_2O_2Se_2(Se_2P^{i}Pr_2)_2]$. *Chem. Commun.* **2006**, 2182–2184.
37. Nguyen, C.; Afzaal, M.; Malik, M. A.; Helliwell, M.; Raftery, J.; O'Brien, P. Novel Inorganic Rings and Materials Deposition. *J. Organomet. Chem.* **2007**, *692*, 2669–2677.
38. Malik, M. A.; Afzaal, M.; O'Brien, P. Precursor Chemistry for Main Group Elements in Semiconducting Materials. *Chem. Rev.* **2010**, *110*, 4417–4446.
39. Akhtar, J.; Afzaal, M.; Vincent, M. A.; Burton, N. A.; Raftery, J.; Hillier, I. H.; O'Brien, P. Understanding the Decomposition Pathways of Mixed Sulfur/Selenium Lead Phosphinato Complexes Explaining the Formation of Lead Selenide. *J. Phys. Chem. C* **2011**, *115*, 16904–16909.
40. Pitts, J.; Robinson, M.; Trotz, S. The Characteristics of Several New Metal Phosphinate Complexes. *J. Inorg. Nucl. Chem.* **1968**, *30*, 1299–1308.
41. Dakternieks, D. Phosphorus-31 and Cadmium-113 NMR Studies of Cadmium (II) Complexes with Some Tertiary Phosphines. *Aust. J. Chem.* **1982**, *35*, 469–481.
42. Yu, W.; Qu, L.; Guo, W.; Peng, X. Experimental Determination of the Extinction Coefficient of CdTe, CdSe, and CdS Nanocrystals. *Chem. Mater.* **2003**, *15*, 2854–2860.
43. Cao, Y. C.; Wang, J. One-Pot Synthesis of High-Quality Zinc-Blende CdS Nanocrystals. *J. Am. Chem. Soc.* **2004**, *126*, 14336–14337.
44. Joo, J.; Na, H.; Yu, T.; Yu, J.; Kim, Y.; Wu, F.; Zhang, J.; Hyeon, T. Generalized and Facile Synthesis of Semiconducting Metal Sulfide Nanocrystals. *J. Am. Chem. Soc.* **2003**, *125*, 11100–11105.
45. Liu, X.; Jiang, Y.; Lan, X.; Li, S.; Wu, D.; Han, T.; Zhong, H.; Zhang, Z. Synthesis of High Quality and Stability CdS Quantum Dots with Overlapped Nucleation-Growth Process in Large Scale. *J. Colloid Interface Sci.* **2011**, *354*, 15–22.
46. Ouyang, J.; Kuijper, J.; Brot, S.; Kingston, D.; Wu, X.; Leek, D. M.; Hu, M. Z.; Ripmeester, J. A.; Yu, K. Photoluminescent Colloidal CdS Nanocrystals with High Quality *via* Noninjection One-Pot Synthesis in 1-Octadecene. *J. Phys. Chem. C* **2009**, *113*, 7579–7593.
47. Kuznetsova, N. A.; Kaliya, O. L. The Photochemistry of Coumarins. *Russ. Chem. Rev.* **1992**, *61*, 683.
48. Qu, L.; Peng, X. Control of Photoluminescence Properties of CdSe Nanocrystals in Growth. *J. Am. Chem. Soc.* **2002**, *124*, 2049–2055.

49. Du, J.; Rettig, S.; Thompson, R.; Trotter, J. Structure of a Polymeric Cadmium Complex Containing Triply Bridging Monophenylphosphinate Ligands. *Acta Crystallogr. C* **1992**, *48*, 1394–1397.
50. Cardoso, M. R. S. Synthesis and Structural Analysis of New Coordination Polymer and Molecular Compounds of Phosphinatos Metals. Ph.D. Thesis, Federal University of Santa Maria, Santa Maria, Brazil, 2007.
51. Owen, J. S.; Park, J.; Trudeau, P.-E.; Alivisatos, A. P. Reaction Chemistry and Ligand Exchange at Cadmium-Selenide Nanocrystal Surfaces. *J. Am. Chem. Soc.* **2008**, *130*, 12279–12281.
52. Attempts to quantify the yield of tetradecanoic anhydride with ^{1}H and ^{13}C NMR and FT-IR spectroscopies was made difficult by low signal-to-noise, high background signals, and the instability of tetradecanoic anhydride under the reaction conditions. FT-IR proved most useful, allowing us to detect >50% of the expected yield of tetradecanoic anhydride.
53. Assuming stoichiometries similar to those found for carboxylate-terminated cadmium selenide nanocrystals, ~0.2 equiv of additional cadmium tetradecanoate is required.
54. Xie, R.; Li, Z.; Peng, X. Nucleation Kinetics *vs.* Chemical Kinetics in the Initial Formation of Semiconductor Nanocrystals. *J. Am. Chem. Soc.* **2009**, *131*, 15457–15466.
55. Chan, E. M.; Xu, C.; Mao, A. W.; Han, G.; Owen, J. S.; Cohen, B. E.; Milliron, D. J. Reproducible, High-Throughput Synthesis of Colloidal Nanocrystals for Optimization in Multidimensional Parameter Space. *Nano Lett.* **2010**, *10*, 1874–1885.
56. Chen, O.; Chen, X.; Yang, Y.; Lynch, J.; Wu, H.; Zhuang, J.; Cao, Y. C. Synthesis of Metal-Selenide Nanocrystals Using Selenium Dioxide as the Selenium Precursor. *Angew. Chem., Int. Ed.* **2008**, *47*, 8638–8641.
57. Benzene, toluene, pentane, hexane, 1-octadecene, acetonitrile, tetrahydrofuran, diethyl ether, chloroform.
58. Empedocles, S. A.; Bawendi, M. G. Influence of Spectral Diffusion on the Line Shapes of Single CdSe Nanocrystallite Quantum Dots. *J. Phys. Chem. B* **1999**, *103*, 1826–1830.